PAIN®

The rostromedial tegmental nucleus: a key modulator of pain and opioid analgesia

Norman E. Taylor[a,*], Hu Long[b,d], JunZhu Pei[c], Phanidhar Kukutla[d], Anthony Phero[a], Farnaz Hadaegh[d], Ahmed Abdelnabi[d], Ken Solt[d], Gary J. Brenner[d]

Abstract

A recently defined structure, the rostromedial tegmental nucleus (RMTg; aka tail of the ventral tegmental area [VTA]), has been proposed as an inhibitory control center for dopaminergic activity of the VTA. This region is composed of GABAergic cells that send afferent projections to the ventral midbrain and synapse onto dopaminergic cells in the VTA and substantia nigra. These cells exhibit μ-opioid receptor immunoreactivity, and in vivo, ex vivo, and optogenetic/electrophysiological approaches demonstrate that morphine excites dopamine neurons by targeting receptors on GABAergic neurons localized in the RMTg. This suggests that the RMTg may be a key modulator of opioid effects and a major brake regulating VTA dopamine systems. However, no study has directly manipulated RMTg GABAergic neurons in vivo and assessed the effect on nociception or opioid analgesia. In this study, multiplexing of GABAergic neurons in the RMTg was achieved using stimulatory Designer Receptors Exclusively Activated by Designer Drugs (DREADDs) and inhibitory kappa-opioid receptor DREADDs (KORD). Our data show that locally infused RMTg morphine or selective RMTg GABAergic neuron inhibition produces 87% of the maximal antinociceptive effect of systemic morphine, and RMTg GABAergic neurons modulate dopamine release in the nucleus accumbens. In addition, chemoactivation of VTA dopamine neurons significantly reduced pain behaviors both in resting and facilitated pain states and reduced by 75% the dose of systemic morphine required to produce maximal antinociception. These results provide compelling evidence that RMTg GABAergic neurons are involved in processing of nociceptive information and are important mediators of opioid analgesia.

Keywords: RMTg, DREADDs, Dopamine, GABA, Opioid analgesia, Nociception

1. Introduction

Despite years of study, the mechanisms responsible for the rewarding and analgesic effects of opioids are incompletely understood, as current knowledge has been insufficient to enable development of potent analgesics that lack the rewarding effects of opioids. Currently, it is known that dopamine neurons in the ventral tegmental area (VTA) contribute to both the analgesic and rewarding properties of opioids, but it is not known whether one property can be separated from the other.[10,26,44]

A recently defined structure, the rostromedial tegmental nucleus (RMTg; aka tail of the VTA), has been proposed as an

inhibitory control center for dopaminergic activity of the VTA.[2,4] This region is composed of GABAergic cells that send afferent projections to the ventral midbrain and synapse onto dopaminergic cells in the VTA and substantia nigra.[9,15,19,33] These cells uniquely exhibit dense μ-opioid receptor immunoreactivity,[16] suggesting they play an important role in opioid function.

The VTA contains a mixture of cell types, including dopaminergic (~65%), GABAergic (~30%), and glutamatergic (~5%) neurons that project to the amygdala, prefrontal cortex, and nucleus accumbens (NAc).[8] For many years, binding to and inhibition of GABAergic interneurons in the VTA was the accepted mechanism by which opioids induced dopamine release from the VTA, owing to the observation that opioids excite dopamine neurons in vitro by hyperpolarization of local GABAergic interneurons.[18] However, a recent study demonstrated that injection of nanomolar quantities of μ-opioid receptor agonists had no effect when injected into the VTA but produced analgesia when injected into the RMTg,[17] suggesting that the RMTg may be a more potent modulator of opioid effects on VTA function.

Multiple recent electrophysiological studies demonstrate that morphine excites dopamine neurons by targeting receptors on GABAergic neurons localized in the RMTg.[14,23,24,27] However, much less is known about the behavioral effects of these findings. No study has yet directly manipulated RMTg GABAergic neurons in vivo and assessed the effect on nociception or opioid analgesia.

We hypothesized that the RMTg is a key center for opioid-mediated antinociception and tested this hypothesis by comparing the analgesic effects of systemic morphine with local RMTg administration. We then used a chemogenetic approach to directly and selectively manipulate GABA neurons of the RMTg to

assess the analgesic potential of these neurons in the context of persistent inflammatory pain. Fast-scan cyclic voltammetry (FSCV) was then used in freely behaving mice to demonstrate that RMTg GABA neurons can modulate dopamine levels in the NAc, and finally, that direct VTA dopamine neuron activation could recapitulate the antinociceptive effects seen with selective RMTg GABA neuron inhibition.

2. Methods

This article adheres to the applicable ARRIVE guidelines.

2.1. Animal care

All animal procedures were reviewed and approved by the Massachusetts General Hospital Institutional Animal Care and Use Committee. Adult male vGat-ires-Cre mice (Jackson Laboratory, stock number 016962) and DAT-cre mice (Jackson Laboratory, stock number 006660) were used for all experiments. Mice were kept on a 12:12-hour light–dark cycle (lights on at 7 AM and lights off at 7 PM) with ad libitum access to food and water. Mice had a minimum of 3 weeks to recover after surgery, and at least 3 days of rest were provided after each experiment.

2.2. Surgery

All mice were anesthetized with 2% isoflurane and placed in a stereotaxic frame (David Kopf Instruments, Tujunga, CA). An incision was made in the skin, and craniotomies were made above the target region. vGat-cre mice received bilateral viral injections using a motorized stereotaxic injector (Stoelting, Wood Dale, Wood Dale, IL) targeting the RMTg (-3.9 mm anterior/posterior, ±0.4 mm lateral, and -4.8 mm dorsal/ventral to the bregma), with 200 nL of a mixture of adeno-associated viruses (AAVs) containing both the AAV8-hSyn-DIO-hM3D(Gq)-mCherry (excitatory, hM3) and AAV8-hSyn-DIO-HA-KORD-mCitrine (inhibitory, KORD) vectors. Control animals were prepared with a virus containing only a fluorescent tag without a receptor (AAV8-hSyn-DIO-mCherry; UNC vector core, Chapel Hill, NC). Dat-cre mice received bilateral injections with the same virus combinations targeting the VTA (-3.4 mm anterior/posterior, ±0.5 mm lateral, and -4.4 mm dorsal/ventral to the bregma). The mice were then allowed to recover for 3 weeks to allow for optimal viral expression.

On completion of all behavioral studies, 3 of the Designer Receptors Exclusively Activated by Designer Drugs (DREADD)/KORD vGat-cre mice were implanted with carbon fiber electrodes for the measurement of dopamine transients in the NAc. Briefly, mice were anesthetized with 2% isoflurane and placed in a stereotaxic frame. In the first group of mice, a craniotomy was performed above the NAc (Anterior/posterior, $+1.0$ mm; medial/lateral, ±1.0 mm), and an Ag/AgCl reference electrode were implanted in the contralateral forebrain. A carbon fiber electrode (~100 μm in length) was then lowered into the NAc (dorsal/ventral, -4.0 mm) in 0.25-mm intervals for voltammetric recordings.

A separate group of mice was implanted with bilateral infusion cannula targeted to the RMTg (-3.9 mm A/P, ±0.4 mm lateral, and -4.8 mm D/V to the bregma). To achieve this, the cannulae were implanted at 15° angles, with entry at the skull at -3.9 mm A/P, ±1.5 mm lateral.

2.3. Chemogenetic manipulation

Mice were habituated to the pain behavior assessment chambers starting 2 weeks after viral injections. At 3 weeks after injection, baseline measurements were obtained by measuring paw withdrawal latencies in 5-minute intervals over 20 minutes. The mice were then randomized to receive intraperitoneal (i.p.) injections of saline, clozapine-N-oxide (CNO, 1 mg/kg; C0832-Sigma-Aldrich, Milwaukee, MI), or salvinorin-B (SB, 0.5 mL @ 15 mg/kg dissolved in 100% DMSO, 75250 Sigma-Aldrich) in a blinded fashion. The mice were then placed back within their individual Plexiglas compartments for 30 minutes before beginning the behavioral assessment. Duplicate paw withdrawal latencies were collected 5 minutes apart. In experiments testing for effects on morphine analgesia, morphine was then administered i.p., followed 15 minutes later by duplicate paw withdrawal latencies, followed immediately by the next dose of morphine. This procedure was repeated until the last dose of morphine was administered. Doses were assumed to be cumulative.

2.4. Inflammatory pain model

To induce a model of persistent inflammatory arthritic pain, a group of DREADD/KORD-prepared vGat-cre mice along with controls was prepared by injecting the left hind ankle of each mouse with complete Freund's adjuvant (CFA, 25 μL of a 20 mg/mL solution, C1013—Sigma-Aldrich dissolved in normal saline) as previously described.[13] Interarticular injection of CFA sensitizes the animal to a thermal stimulation, an effect that lasts for about 4 weeks in the doses administered. Two weeks after the CFA injection, paw withdrawal latencies were tested in the inflamed paw and the contralateral uninflamed paw to establish the presence of CFA-induced inflammatory pain. Both vGat-cre mice and DAT-cre mice were treated with either CNO (1 mg/kg) or SB (15 mg/kg) in a blinded fashion, followed 30 minutes later by treatment with morphine. Seven days later, the procedure was repeated, with each animal receiving the drug that was not administered the week before. Seven days after that, animals were tested for conditioned place preference (CPP). After these studies, 3 DREADD/KORD mice were used for FSCV, 2 animals were used for slice electrophysiology, and the remaining brains were harvested for histologic testing.

2.5. Pain behavioral testing

To evaluate nociception, thermal withdrawal latencies were assayed as previously described.[36] The Hargreaves test was performed to evaluate heat sensitivity thresholds, measuring latency of withdrawal to a radiant heat source (IITC Life Science, Model 390). We applied the radiant heat source to both the hind paws sequentially and measured the latency to evoke a withdrawal. Two to five replicates were acquired per hind paw per mouse, and values for both paws were averaged.

2.6. Conditioned place preference

We used a modification of standard CPP protocols.[25,28] In brief, animals were habituated to the CPP apparatus for 1 day, underwent pretesting to assess for any preference, then conditioning trials were conducted daily for the next 6 days. On each of these days, mice underwent SB and vehicle pairing in separate sessions. The following day, CPP was assessed by placing mice in a central chamber and then measuring time spent in the SB-paired and vehicle-paired chamber.

2.7. Locomotion testing

After thermal nociception testing, mice were individually placed into the center of an open-field test environment of clear acrylic

plastic (40 × 40 × 40 cm). Their movements were recorded for 5 minutes using a USB camera and video-tracking system (Any-Maze; Stoetling Co).

A rotating rod apparatus (Columbus Instruments, Columbus, OH) was also used to assess motor performance as described previously.[35] Mice were placed on the elevated accelerating rod beginning at 1 rpm/minute for 2 trials. Each trial lasted 3 minutes, during which time the rotating rod underwent a linear acceleration from 1 to 40 rpm. Animals were scored for their latency (in seconds) to fall in each trial, and the average of 2 trials is reported. Animals rested a minimum of 10 minutes between trials to avoid fatigue.

2.8. Fast-scan cyclic voltammetry

Fast-scan cyclic voltammetry experiments were conducted using a previously described method.[42] Before implantation, the carbon fiber electrodes were calibrated in vitro with known concentrations of dopamine (0.2, 0.5, and 1.0 μM). After implantation, baseline voltammetric measurements were taken by applying a triangle waveform (−0.4 to +1.1 to −0.4 V vs Ag/AgCl, at 400 V/second) to the carbon fiber electrode every 100 ms. Data were digitized and recorded in a PC using Pinnacle's FSCV software in its extended continuous mode. This software was also used to apply the triangle waveform, background subtract voltammograms, and generate voltammo-gram heat maps, single-sweep voltammograms, and quantitative dopamine graphs. Heat maps in this software are plotted by time vs a voltage index, rather than the voltage sweep (−0.4 to 1.1 to −0.4 V), as is most commonly depicted in the literature. A dopamine transient was defined as a change in current equivalent to a 30-nM change in dopamine concentration in voltammetric signals, displaying an oxidation peak at +0.65 V and a reduction peak at −0.2 V as well as the characteristic cyclic voltammogram (CV) shape.

Chemical identification of signals was performed by examining background-subtracted CVs. The subtraction process yields changes in concentration that cannot be used to establish absolute levels.[34] To isolate dopamine transients, a "sliding background" subtraction was initially used. In this approach, each CV in a 2-minute file was subtracted from the average of the 5 CVs collected 1.0 to 0.5 seconds earlier, and the resulting CV compared with a calibration CV. In addition, a Principal Component Regression method was used to remove electrode drift and quantitatively separate dopamine transients from noise, as described previously.[20] Only voltammograms with an $r^2 > 0.30$ were considered dopamine; the remainder of the signal was considered noise.

Mice were habituated for 30 minutes before the 25 minutes of baseline recording in freely behaving mice. The vGat-cre mice were then administered D-amphetamine (3 mg/kg) i.p., and FSCV data were collected for an additional 55 minutes to test the effectiveness of the probes. Mice that showed an increase in NAc dopamine release were subsequently tested in 3-day intervals with either CNO (1 mg/kg) or SB (15 mg/kg) in a random, blinded fashion. On completion of the experiments, DREADD/KORD expression and fiber tip location were verified histologically.

2.9. Immunohistochemistry

After all experiments were completed, viral expression and localization was verified through histological analysis. Dat-cre animals were perfused with phosphate-buffered saline followed by neutral buffered formalin. The brains were postfixed in formalin

overnight and then sliced at 50 μm using a Leica VT1200 S vibratome (Leica Microsystems Inc, Buffalo Grove, IL). Specific expression of DREADDs in DA neurons was confirmed by colocalization of mCherry (from AAV expression) with immuno-histochemical staining for tyrosine hydroxylase, a marker of dopamine neurons (mouse anti-TH, 1:1000 dilution, Millipore Cat #MAB318, Temecula, CA) using the secondary antibody of goat anti-mouse conjugated to Alexa 488 (1:200 dilution, catalog no. A-11001; Invitrogen, Waltham, MA). Cells were counterstained with 4′,6-diamidino-2-phenylindole (DAPI, catalog no. H-1200 Vectashield) for nuclear visualization. Images were taken with a Zeiss Axio M2 microscope (Zeiss, Oberkochen, Germany). Confirmation of viral expression in the correct brain region was performed by comparing images with a Mouse Brain Atlas.[32] On histologic verification, it was discovered that the KORD virus did not express in DAT-cre mice. Therefore, no behavior data were presented in DAT-cre mice receiving SB. Identification of vGat protein in vGat-cre mice was also initially attempted using immunohistochemistry. However, we could not find an antibody that could clearly demonstrate colocalization. We therefore elected to perform fluorescence in situ hybridization (FISH) on histologic samples from vGat-cre mice to show viral expression in vGat-containing neurons.

2.10. Fluorescence in situ hybridization

Brains from 2 mice were swiftly harvested and immediately flash frozen in a beaker filled with a bilayer of 1-methylbutane and 1-bromobutane on dried iced and subsequently stored at −80°C. The brains were sectioned on a cryostat and mounted on Superfrost Plus Gold slides (25 × 75 mm; Erie Scientific, Ramsey, MN). One hour before sectioning, brains and slides were equilibrated to −20°C in the cryostat. The specified brains were serially sectioned coronally at 14 μm and mounted onto slides through the warmth of the hand. The mounted specimens were dried for 1 hour inside the cryostat and then stored at −80°C.

Double-label fluorescence in situ hybridization was performed using RNAScope Manual Fluorescent Multiplex Kit User Manual specified for Fresh Frozen Tissue (Advanced Cell Diagnostics). Slides were fixed in 4% paraformaldehyde at 4°C, serially dehydrated, washed twice in phosphate-buffered saline pH 7.38, and pretreated with protease IV solution for 15 minutes. Specimens were then incubated with target probes for mouse vglut2 (*slc17a6* target region 1986-2998, catalog no. 319171, Advanced Cell Diagnostics) and mCherry (*mcherry* target region 23-681, catalog no. 431201-C2, Advanced Cell Diagnostics). Next, the slides underwent 4 serial amplification incubations, the last of which contained fluorescent probes (Alexa 488 and Atto 550 catalog no. 320850 Advanced Cell Diagnostics Part of Florescent Multiplex Kit) individually targeted to the slc17a6 and mCherry probes. Finally, the slides were mounted with ProLong Diamond Antifade Mountant with DAPI (catalog no. P36962, Invitrogen). Images were taken with a Zeiss Imager M2 microscope (Zeiss).

2.11. Statistical analysis

GraphPad Prism was used to perform all graphical and statistical analyses. The number of mice used for each group (n) is reported both in the text and in the figure legends. All paw withdrawal latency values are reported and graphically depicted as mean values with 95% confidence intervals (CIs), whereas the differences in the time spent in the drug-paired chamber before and after conditioning in the CPP experiment are graphically depicted

as medians with 95% CIs. Data were first tested for normality using a Shapiro–Wilk test. Parametric experimental and control data were then analyzed using a 2-way ANOVA to test for significance. Differences were deemed to be significant with P values < 0.05. Nonparametric data were then analyzed using the Friedman test for one-way repeated-measures analysis of variance by ranks, with P < 0.05 deemed to be significant. Subsequently, multiple t tests were conducted using a Holm–Sidak method to correct for the multiple comparisons, with alpha = 0.05.

For the FSCV experiment, data were analyzed in 20-second segments to determine the presence or absence of dopamine transients. The frequency of dopamine transients was then graphically reported as the rate of dopamine transients per minute. Differences from baseline were tested for significance by averaging the first 20 minutes of baseline data, and comparing this average with the postinjection mean obtained by averaging the data between minutes 40 and 60. Data were first tested for normality using a Shapiro–Wilk test. The nonparametric data were then analyzed using the Friedman test for one-way repeated-measures analysis of variance by ranks, with P < 0.05 deemed to be significant.

3. Results

DREADD-mediated selective inhibition and activation of RMTg GABAergic neurons was used to investigate whether these cells have a role in nociception and analgesia. Adult male mice expressing Cre recombinase in GABAergic cells carrying the vesicular GABA transporter (vGat-ires-Cre) underwent bilateral RMTg injection of an AAV carrying both the inhibitory G_i-coupled SB-activated KORD and the stimulatory, G_q-coupled, CNO-activated hM3Dq receptor (DREADD/KORD, n = 8). Control mice were similarly prepared but differed in that the RMTg was injected with a viral construct lacking any G-protein-coupled receptors (control, n = 5) (**Figs. 1A and B**). Expression was restricted to cell
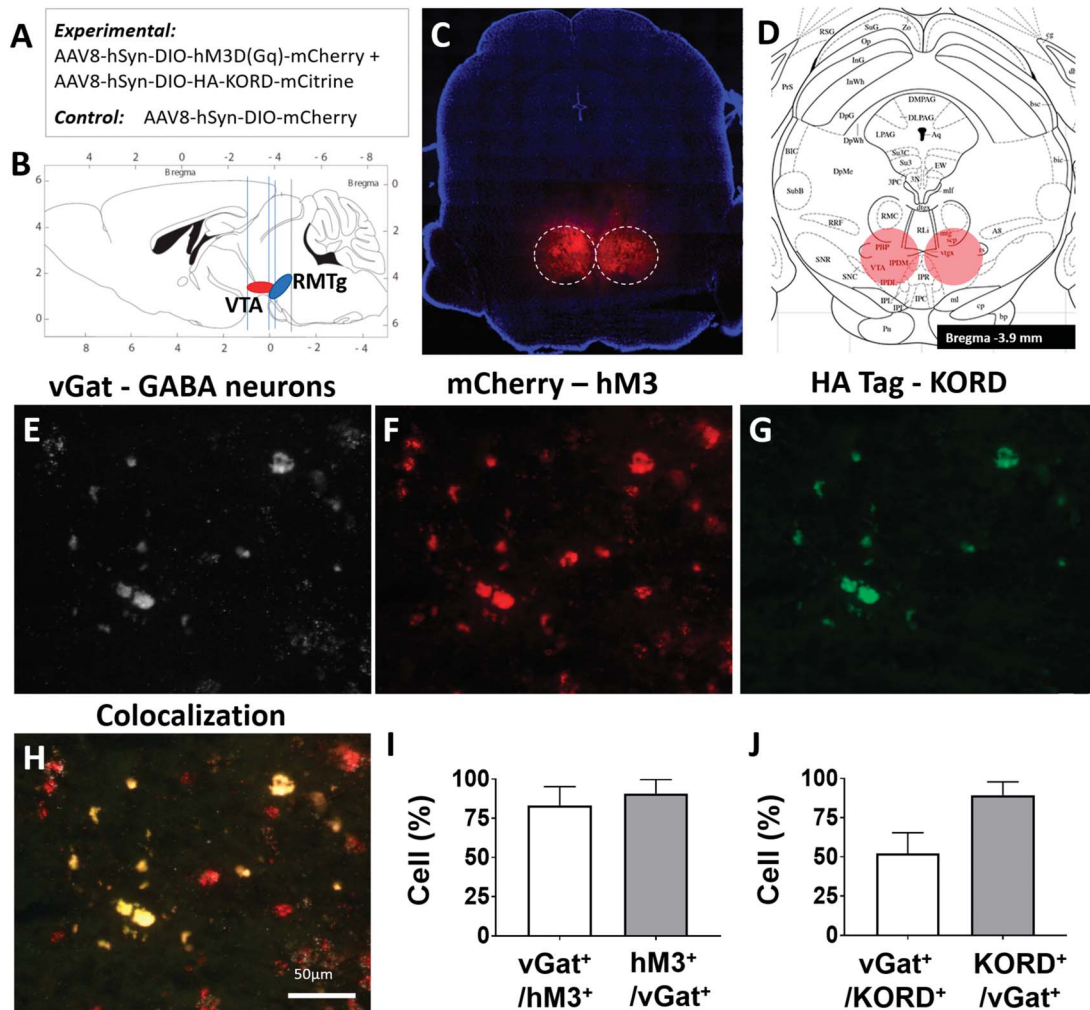

Figure 1. Validation studies demonstrate localization and functionality of RMTg-targeted hM3 DREADDs and KORD. (A) Summary of cre-dependent viral constructs delivered to the RMTg. (B) Orientation and proximity of the RMTg in relation to the VTA. (C) AAV-hsyn-DIO-hM3D(Gq)-mCherry expression in the RMTg of a representative vGat-cre mouse (see also Fig. S1, available online as supplemental digital content at http://links.lww.com/PAIN/A842). (D) RMTg target location on the mouse atlas (−3.9 mm anterior/posterior, ±0.4 mm lateral, and −4.8 mm dorsal/ventral to the bregma). (E) Fluorescence in situ hybridization (FISH) staining of the vesicular GABA transporter (vGat) in RMTg neuronal cell bodies in a representative mouse. (F) hM3D-mCherry expression in the same region as (E). (G) HA tag (KORD) expression in the same region as (E). (H) Overlayed image of (E, F, and G) showing colocalization of hM3D and KORD expression in vGat-expressing neurons of the RMTg; scale bar, 50 μm. (I) 91 ± 6% of red-labelled hM3D$^+$ transcripts in the RMTg colocalized with white, Cy5-labeled neurons expressing vGat RNA, and 83 ± 8% of white Cy5-labelled vGat-cre–expressing neurons colocalized with red, mCherry-labelled hM3D$^+$ transcripts. (J) 90 ± 9% of green-labelled KORD$^+$ transcripts in the RMTg colocalized with white, Cy5-labeled neurons expressing vGat RNA, and 52 ± 13% of white Cy5-labelled vGat-cre–expressing neurons colocalized with green-labelled KORD$^+$ transcripts. RMTg, rostromedial tegmental nucleus; VTA, ventral tegmental area.

bodies in the RMTg, as shown in **Figures 1C and D**, with additional axonal staining of known RMTg projections in the medial tegmentum, pedunculopontine and laterodorsal tegmental nuclei, dorsal raphe, locus coeruleus, and subcoeruleus.[16] The extent and location of the viral expression in all animals is summarized in Figure S1 (available online as supplemental digital content at http://links.lww.com/PAIN/A842). Fluorescence in situ hybridization demonstrated robust DREADD and KORD expression in the RMTg (**Figs. 1E–G**) that colocalized with neurons expressing vGat RNA (**Fig. 1H**). We observed 91 ± 6% of red-labelled, RMTg hM3$^+$ transcripts colocalized with white, Cy5-labeled neurons expressing vGat RNA, and 83 ± 8% of white Cy5-labelled vGat-cre–expressing neurons colocalized with red, mCherry-labelled hM3D$^+$ transcripts (**Fig. 1I**). 90 ± 9% of green-labelled, RMTg, KORD$^+$ transcripts colocalized with white, Cy5-labeled neurons expressing vGat RNA, and 52 ± 13% of white Cy5-labelled vGat-cre–expressing neurons colocalized with green-labelled KORD$^+$ transcripts (**Fig. 1J**). Based on this histologic examination, no animals were excluded in the behavioral analysis.

Baseline nociceptive and morphine analgesic responses were measured using the Hargreaves method, a well-studied, quantitative test that uses time to foot withdrawal from mild radiant heat ("withdrawal latency") as a measure of thermal nociception.[13] We first tested the effects of systemic morphine administration, and as expected, there was a morphine dose–response effect on thermal withdrawal latency (**Fig. 2A**), with maximal withdrawal latency of DREADD/KORD mice of 19.6 seconds (95% CI 18.1-21.2 seconds) and no difference between mice expressing the DREADD/KORD combination (n = 8) and those that did not (n = 5).

If the RMTg is important in opioid analgesia, then targeted delivery of morphine to the RMTg would also be expected to prolong withdrawal latency to heat. To test this, a separate group of mice (n = 6) was prepared with infusion cannula targeting the RMTg (Fig. S2, available online as supplemental digital content at http://links.lww.com/PAIN/A842). As shown in **Figure 2B**, bilateral intra-RMTg morphine infusion (1 µg/50 nL/side) was effective in producing significantly increased paw withdrawal latency, which peaked at 10 minutes after injection (17.1 seconds 95% CI [11.9-22.2 seconds], $P = 0.0004$). Injections in 2 mice were determined to be unilateral based on histologic confirmation of the cannula tip locations (Fig. S2, available online as supplemental digital content at http://links.lww.com/PAIN/A842). No difference was seen in the analgesic response to morphine between animals receiving unilateral or bilateral RMTg injections.

Because of the close physical proximity of the VTA and the RMTg, we elected to use a chemogenetic approach to selectively target RMTg GABAergic neurons to further assess their effects on thermal hyperalgesia. As shown in **Figure 2C**, RMTg GABAergic neuron inhibition (SB) significantly increased paw withdrawal latency, indicating antinociception, whereas activation (CNO) significantly decreased hind paw withdrawal latency to thermal stimulation, indicating nociceptive sensitization. Interestingly, the increase in heat withdrawal latency achieved by local RMTg morphine injection (17.1 seconds 95% CI [11.9-22.2 seconds]) and that achieved by selective RMTg GABAergic neuron inhibition (17.1 seconds 95% CI [14.55-19.73 seconds]) were nearly identical and were equivalent to 87% of the maximal analgesic effect of systemic morphine. The magnitude of these effects was unexpected and indicates that the RMTg has an important role in both nociception and morphine analgesia. A modulatory role of RMTg GABAergic neurons in morphine analgesia was further supported by our demonstration that RMTg GABAergic neuron inhibition (SB) significantly enhanced
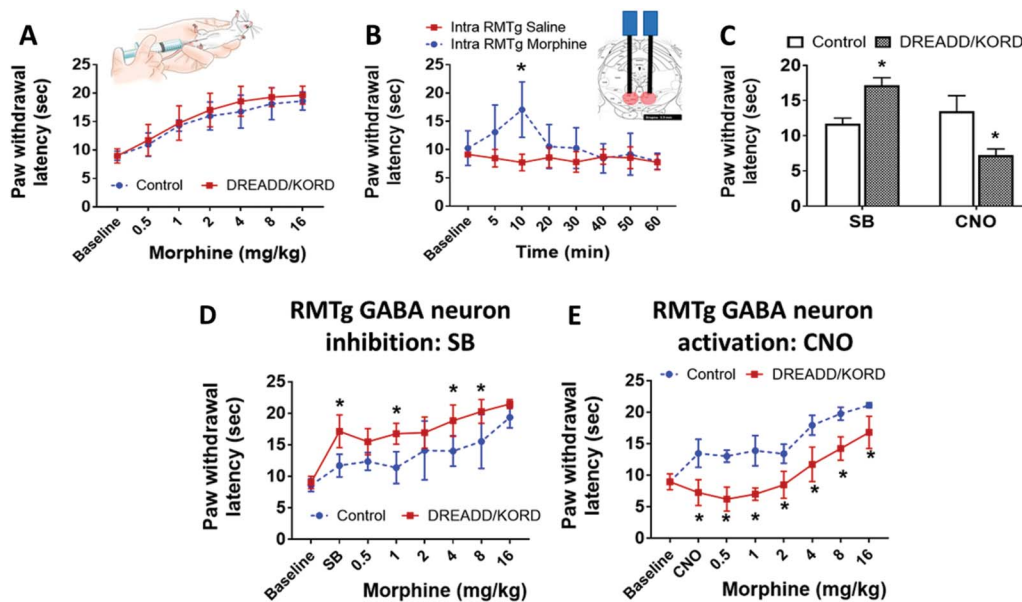

Figure 2. Local RMTg morphine administration and direct RMTg GABA neuron inhibition produce antinociception. (A) Effect of systemic morphine administration on paw withdrawal latency to a thermal stimulus in vGat-cre mice expressing hM3D/KORD in the RMTg (DREADD/KORD) or controls lacking the receptors (Control). Mean (±95% CI). (B) Effect of local RMTg morphine administration (1 µg/50 nL/side) or saline on paw withdrawal latency to a thermal stimulus. Mean (±95% CI), * $P = 0.0004$, 2-way ANOVA (see also Fig. S2 available online as supplemental digital content at http://links.lww.com/PAIN/A842). (C) Effect of intraperitoneal (i.p.) salvinorin-B (SB) and clozapine-N-oxide (CNO) on paw withdrawal latency to a thermal stimulus in vGat-cre mice expressing hM3D/KORD in the RMTg (DREADD/KORD) or controls lacking the receptors (Control). Mean (±95% CI), *$P < 0.001$, 2-way ANOVA. (D) Effect of i.p. SB on morphine antinociception in vGat-cre mice expressing hM3D/KORD (DREADD/KORD) or controls lacking the receptors (Control). Mean (±95% CI), *$P < 0.01$, t tests with the Holm–Sidak correction. (E) Effect of i.p. CNO on morphine antinociception in the same mice as (D). Mean (±95% CI), *$P < 0.05$, t tests with the Holm–Sidak correction. CI, confidence interval; RMTg, rostromedial tegmental nucleus.

analgesic effects of systemic morphine (**Fig. 2D**), whereas activation (CNO) significantly inhibited this morphine effect (**Fig. 2E**). These properties existed across the entire range of a morphine dose–response curve.

To test whether RMTg GABAergic neuron inhibition could modulate nociceptive responses in a facilitated pain state, persistent inflammatory pain was generated by injecting CFA into the left ankle joint of DREADD/KORD-prepared vGat-cre mice along with controls. Three weeks after CFA injection, hind paw withdrawal latency to thermal stimulation in KORD− (P = 0.0059) and KORD+ (P = 0.0041) mice was significantly reduced compared with pre-CFA values, indicating inflammation-associated nociceptive sensitization had been generated (**Fig. 3A**). Salvinorin-B injection had no effect in KORD− mice (P = 0.80) but significantly increased paw withdrawal latencies in KORD+ mice (P = 0.0009), suggesting that RMTg GABA neuron inhibition had a significant antinociceptive effect in the context of inflammatory sensitization. Paw withdrawal latencies increased significantly in both KORD− and KORD+ mice, with RMTg GABA inhibition by SB equivalent in magnitude to approximately 45% of the maximal morphine effect. By contrast (**Fig. 3B**), there was no significant change in paw withdrawal latencies when CNO was administered in DREADD+ mice (P = 0.43) sensitized by CFA-induced inflammation.

It has been suggested that operant behavioral tests may be a more clinically relevant endpoint than tests of nocifensive responses (eg, Hargreaves) for the assessment of analgesic responses in rodents.[29] We therefore used CPP to assess whether modulation of RMTg GABAergic neurons regulates stimulus-independent pain. On 5 consecutive days, we paired SB injection with the light enclosure for experimental and control mice, which had undergone left ankle joint CFA injection at least 2 weeks before testing.[25,28] On the sixth day, mice were allowed to freely explore the place-preference apparatus containing a light and a dark enclosure, and the time spent in each enclosure was measured. We found that CPP to SB treatment developed in mice expressing DREADD/KORD in RMTg GABAergic neurons, but not in similarly treated control mice (**Fig. 3C**). Using an analogous experimental paradigm, neither CPP nor conditioned place aversion developed in CNO-treated mice (**Fig. 3D**). These CPP data were consistent with the Hargreaves data and demonstrated that SB-induced RMTg GABAergic inhibition reduced both stimulus-dependent (noxious heat/Hargreaves test) and stimulus-independent pain (CFA-induced inflammatory pain/CPP).

As impairment of motor function would confound results of the Hargreaves and CPP tests, we investigated the consequences of RMTg GABA neuron modulation on locomotion. Salvinorin-B–induced inhibition of RMTg GABA neurons had no effect on motor performance in either open-field or rotarod tests, whereas CNO activation of these neurons significantly impaired performance (ie, decreased fall latency) in the rotarod test and decreased distance travelled in the open-field test (Fig. S3,
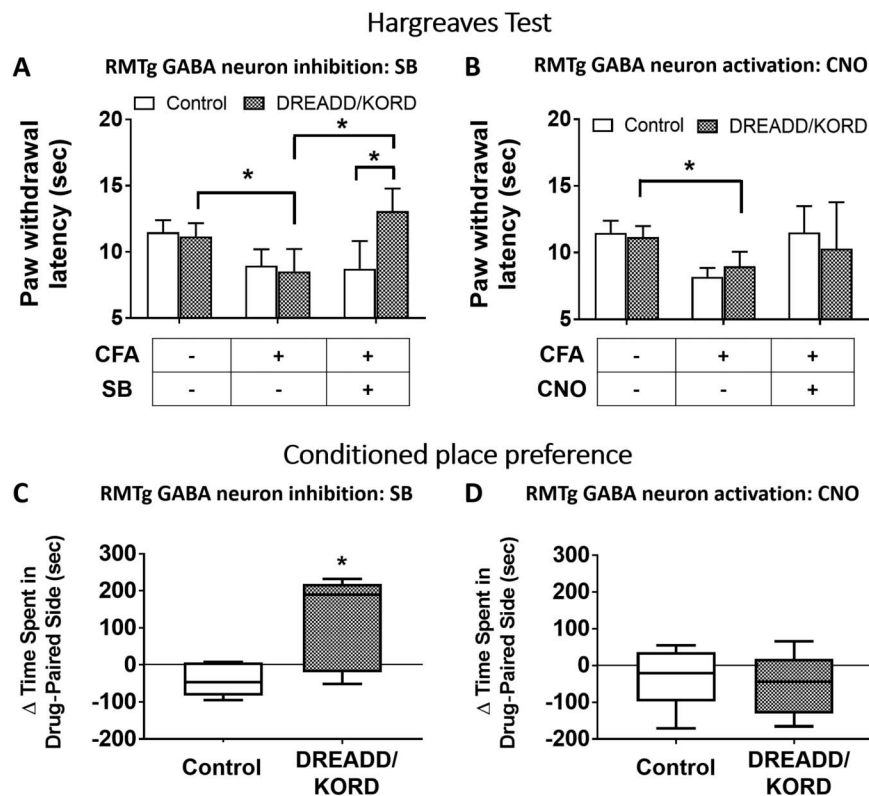

Figure 3. Direct RMTg GABA neuron inhibition is antinociceptive and diminishes both stimulus-dependent and stimulus-independent inflammatory pain in vGat-cre mice expressing DREADD/KORD in the RMTg, but not in controls lacking the receptors. (A) Salvinorin-B (SB) increases paw withdrawal latency in mice with CFA-induced ankle joint inflammation that express KORD in the RMTg. Mean (±95% CI). (B) Clozapine-N-oxide (CNO) has no effect on paw withdrawal latency in mice with CFA-induced ankle joint inflammation that express hM3 DREADD in the RMTg. Mean (±95% CI). *P < 0.01, paired t tests with the Holm–Sidak correction for multiple comparisons. (C) A conditioned place preference developed to SB in mice with CFA-induced ankle joint inflammatory pain in which RMTg GABA neurons were inhibited. Median (±95% CI). (D) A conditioned place preference did not develop to CNO in mice with CFA-induced ankle joint inflammatory pain in which RMTg GABA neurons were excited. Median (±95% CI), *P < 0.01, t tests with the Holm–Sidak correction. CFA, complete Freund adjuvant; CI, confidence interval; RMTg, rostromedial tegmental nucleus.

available online as supplemental digital content at http://links. lww.com/PAIN/A842). Importantly, this indicates that the observed decrease in heat withdrawal latency associated with RMTg GABA neuron inhibition (ie, SB treatment) was not due to depression of sensory-motor function.

We then used FSCV to both (1) assess whether RMTg neurons modulate DA release in the NAc in vivo and (2) validate DREADD activity and function by the presence of expected downstream effects. Fast-scan cyclic voltammetry applies a voltage to a carbon fiber microelectrode, which produces characteristic current/voltage peaks when exposed to DA and can be used to quantitate DA levels by use of a standard curve. Carbon fiber microelectrodes were implanted into the NAc of vGat-cre mice, which had undergone viral injections containing DREADD/KORD targeted to RMTg GABAergic neurons (**Fig. 4A**). One week later, each mouse was administered D-amphetamine (3 mg/kg) i.p. and FSCV data were collected in awake, freely behaving animals to test the effectiveness of the probes. Mice that showed an increase in NAc dopamine transients (n = 3), as shown in **Figure 4B**, were subsequently tested in 3-day intervals with either CNO (1 mg/kg) or SB (15 mg/kg) in a random, blinded fashion. To detect dopamine transients, a voltage ramp was applied to a silver electrode, using parameters depicted in the left panel of **Figure 4C**. This voltage produced a background current as shown in the right panel of **Figure 4C**. Known concentrations of dopamine were used to calibrate the probe, and intensity plots of 20-second interval, background-subtracted, CVs were generated (**Fig. 4D**). A dopamine transient was then defined as a change in current equivalent to a 30-nM change in dopamine concentration in voltammetric signals displaying an oxidation peak at +0.65 V and a reduction peak at −0.2 V (**Fig. 4E**).

One mechanism by which RMTg neurons could mediate morphine analgesia is by inducing DA release by VTA dopaminergic neurons (**Figs. 4F and G**). As shown in **Figure 4H**, inhibition of RMTg GABAergic neurons by i.p. SB injection increased DA transients in the NAc (baseline: 1.35/minute, 95% CI [1.1, 1.7/minute], vs post-SB: 3.65/minute, 95% CI [2.95, 4.38/minute], $P = 4.30e-05$), whereas activation through i.p. CNO administration (**Fig. 4I**) significantly decreased DA transients (baseline: 1.6/minute, 95% CI [1.25, 2.0/minute], vs post-CNO: 0.05/minute, 95% CI [0, 1.5/minute], $P = 5.89e-07$).

If the antinociceptive effect of RMTg GABA neuron inhibition is mediated by excitation of VTA DA neurons, then direct activation of these neurons should also produce analgesia. To test this hypothesis, adult male mice expressing Cre recombinase under the transcriptional control of the DA transporter promoter (DAT-cre mice) underwent targeted injections of AAV carrying an excitatory DREADD (AAV8-hM3Dq, n = 14) or an AAV containing only the mCherry fluorescent tag (n = 9). Immunohistochemistry demonstrated robust DREADD expression restricted to the VTA that colocalized with neurons expressing tyrosine hydroxylase (**Fig. 5A**).

In control mice (VTA DA neurons lacking functional DREADDs), administration of CNO produced no change in hind paw withdrawal latencies compared with baseline, demonstrating that there were no nonspecific CNO effects (**Fig. 5B**). By contrast, CNO activation of VTA DA neurons in DREADD/KORD mice produced profound antinociception (**Fig. 5B**). These mice were then injected with increasing doses of systemic morphine to determine whether the effect of direct DREADD-induced VTA DA neuron activation could be further enhanced. Paw withdrawal latencies failed to increase further with the addition of morphine in DREADD/KORD mice because of a ceiling effect of the assay; VTA DA neuron stimulation by CNO produced an effect equal to

the maximal analgesic effect of systemic morphine. To determine whether VTA DA stimulation would be as effective in modulating heat withdrawal latency in the context of inflammation-induced nociceptive sensitization, CFA was injected into the left hind ankle of 2 groups of mice. Three weeks after CFA injection, the presence of inflammatory pain sensitization was confirmed in both DREADD/KORD and control mice, as paw withdrawal latencies were significantly reduced in the CFA-injected paws compared with the contralateral uninflamed paws in both groups of mice (CFA time point on **Fig. 5C**). As was the case in mice without hind paw inflammation (**Fig. 5B**), CNO greatly increased hind paw withdrawal latencies in DREADD/KORD but not in control mice. However, a slower paw withdrawal latency persisted in the inflamed paw of DREADD/KORD mice. Maximal analgesia, the point at which the paw withdrawal latencies in the inflamed and uninflamed paws became equal, was attained with 2 mg/kg of morphine in DREADD/KORD mice concurrently experiencing VTA DA neuron stimulation, whereas maximal analgesia was attained with 8 mg/kg of morphine in control mice (**Fig. 5C**). This indicates that activation of VTA DA neurons significantly attenuated the thermal hyperalgesia induced by inflammation, and this effect was synergistic with morphine in producing maximal analgesia at approximately a quarter of the systemic morphine dose required to achieve maximal effect.

4. Discussion

In this study, we show that local RMTg morphine and selective RMTg GABAergic neuron inhibition produced 87% of the maximal analgesic effect observed with systemic morphine. Although chemogenetic inhibition of RMTg GABAergic neurons produced antinociception, activation of the same neurons sensitized mice to noxious heat. We also show that the analgesic effects of systemic morphine could be modulated by targeted chemogenetic excitation and inhibition of RMTg GABA neurons. The antinociceptive effect of RMTg GABAergic neuron inhibition was also present in the context of inflammation-induced sensitization as assessed by both nocifensive (hind paw withdrawal) and operant (CPP) behavioral endpoints. Mechanistically, we showed that RMTg GABAergic neurons modulate dopamine release in the NAc, presumably through effects on VTA DA neurons, and that direct activation of VTA dopaminergic neurons produces profound antinociception.

The work presented here supports a critical (but not exclusive) role of the RMTg in nociceptive processing and μ-opioid receptor–mediated analgesia, and further suggests that these RMTg GABA neuron functions are altered in the context of persistent pain. There are many peripheral and central nervous system sites that possess high concentrations of μ-opioid receptors. These sites include the dorsal horn of the spinal cord, periaqueductal gray, lateral parabrachial nucleus, amygdala, and anterior cingulate cortex.[45] μ-Opioid receptors are also found on VTA GABAergic interneurons, which are known to modulate the VTA dopaminergic tone.[18] It is therefore significant that both local RMTg morphine and selective RMTg GABAergic neuron inhibition recapitulate such a high percentage (approx. 87%) of the maximal analgesic effect of systemic morphine. These interventions may not be targeting precisely the same population of GABAergic neurons, as it is possible that not all RMTg GABAergic cells express mu-opioid receptors. However, this strongly suggests that the RMTg is an important site mediating opioid analgesia and supports a previous finding that local infusion of the mu agonist endomorphin-1 into the RMTg markedly reduced formalin-induced pain behaviors.[17]
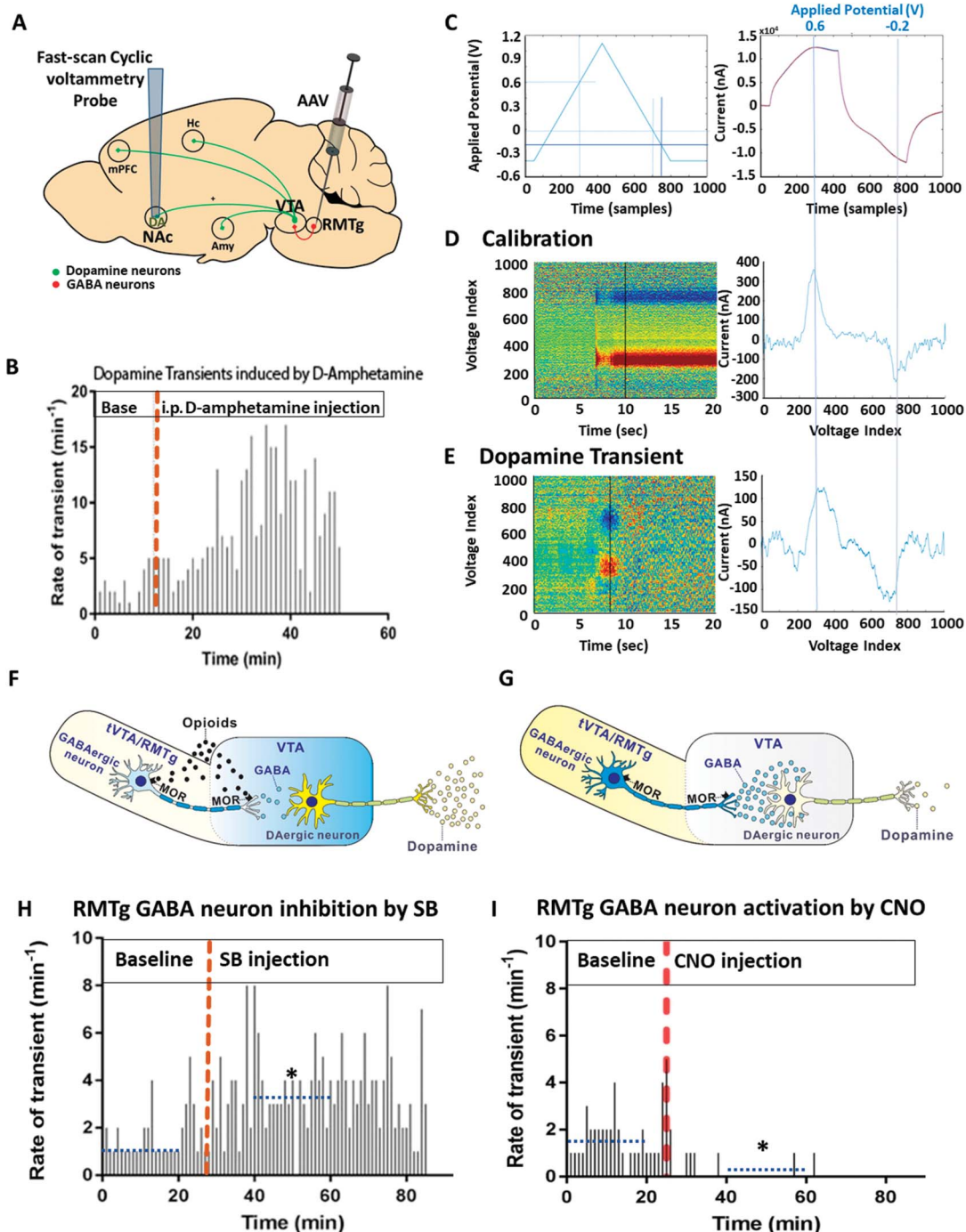
Figure 4. RMTg GABA neurons modulate nucleus accumbens' dopamine levels. (A) Adeno-associated virus (AAV) carrying hM3 DREADDs and KORD was targeted to RMTg GABAergic neurons, whereas carbon-fiber microelectrodes were implanted in the nucleus accumbens (NAc) of vGat-cre mice (n = 3) to measure dopamine transients using fast-scan cyclic voltammetry (FSCV) in freely behaving mice. (B) As a positive control, microelectrode-implanted mice received a 3 mg/kg intraperitoneal (i.p.) injection of D-amphetamine, which resulted in an increase in dopamine transients detected in the NAc. (C) To detect transients, a triangle waveform (−0.4 to +1.1 to −0.4 V vs Ag/AgCl, at 400 V/second) was applied to the carbon fiber electrode every 100 ms. During this time, 1000 samples were taken of the resulting current, and the relationship between the sample number and applied voltage is depicted in the left panel. The right panel shows the background current produced by the applied triangle waveform voltage. The voltage associated with the 300th and the 750th sample is shown at the top of the right graph. (D) Probes were placed into known concentrations of dopamine solution, and the voltage applied to calibrate the probes. Intensity plots were then generated to visualize the resulting current/voltage changes. The left colored panel represents the set of all background-subtracted cyclic voltammograms recorded over a 20-second interval. The right panel shows the individual cyclic voltammogram from the 10-second time point of this set, displaying the expected oxidation peak at +0.65 V and reduction trough at −0.2 V. (E) Dopamine transients recorded in vivo were compared against voltammograms collected during the calibration. A principal component regression method was used to remove electrode drift and quantitatively separate dopamine transients from noise. Only voltammograms with an $r^2 > 0.30$ were considered dopamine. (F) One mechanism through which RMTg neurons could mediate morphine analgesia is by inducing dopamine release by VTA neurons. (G) Conversely, excitation of RMTg GABAergic neurons could decrease dopamine release by VTA neurons. (H) Inhibition of RMTg GABAergic neurons by SB increased dopamine transients in the NAc, (I) whereas activation by CNO significantly decreased dopamine transients (dotted blue line depicts mean value over the indicated 20-minute period, *$P < 0.05$, the Friedman test for one-way repeated-measures analysis of variance by ranks). RMTg, rostromedial tegmental nucleus; VTA, ventral tegmental area.
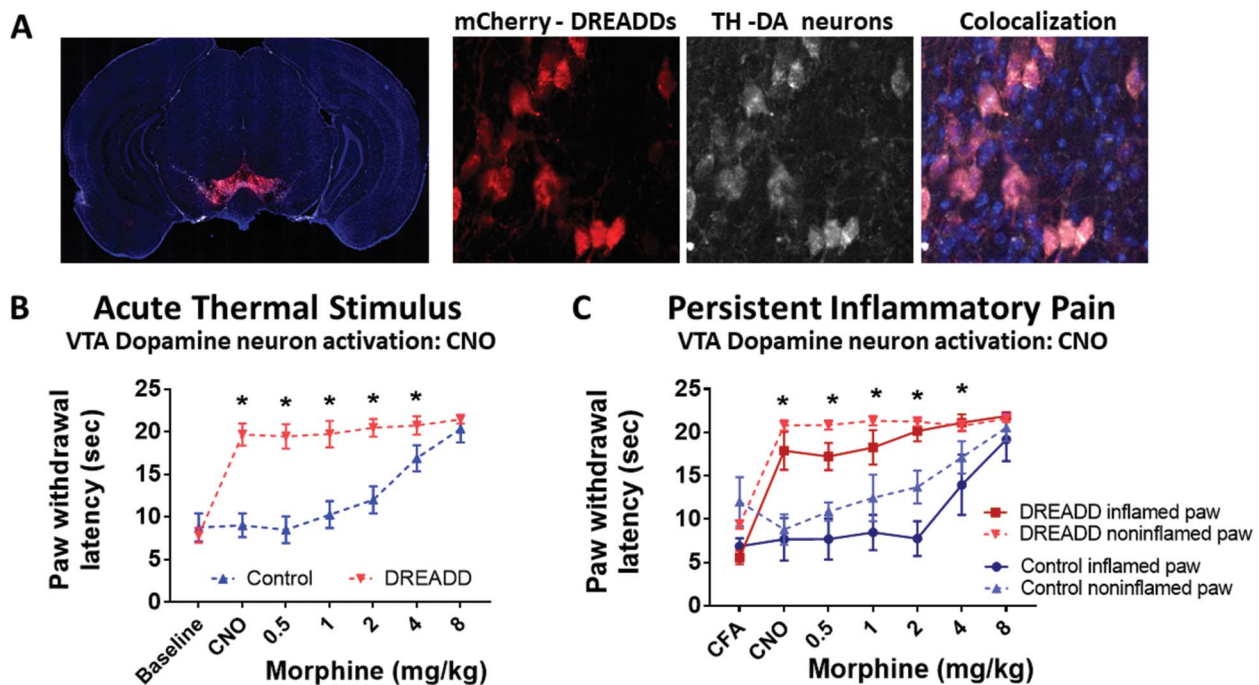
Figure 5. Direct VTA dopamine neuron stimulation is antinociceptive, diminishing both acute thermal and CFA-induced inflammatory pain. (A) AAV-hsyn-DIO-hM3D(Gq)-mCherry expression in the VTA of a representative Dat-cre mouse. hM3D expression is visualized through the red mCherry tag. Immunohistochemical staining of tyrosine hydroxylase (TH) indicating the cell bodies of dopaminergic neurons. The overlayed image showing colocalization of hM3D in TH-expressing neurons of the VTA. (B) Effect of intraperitoneal (i.p.) clozapine-N-oxide (CNO) and morphine on paw withdrawal latency to a thermal stimulus in DAT-cre mice expressing hM3D in the VTA (DREADD) or controls lacking the receptors (Control). Mean (±95% CI), *$P < 0.001$, 2-way ANOVA. (C) Effect of i.p. clozapine-N-oxide (CNO) and morphine on thermal paw withdrawal latency in mice with CFA-induced ankle joint inflammatory pain. Mean (±95% CI). *$P < 0.05$, t tests with the Holm–Sidak correction. CFA, complete Freund adjuvant; CI, confidence interval; VTA, ventral tegmental area.

A concern regarding murine behavioral tests of thermal nociception is that they may be spinally mediated and thus not model "pain" in humans. For example, the tail-flick response has been shown to be a reflex that can be elicited after spinal cord transection.[41] Our results demonstrate that there are central interventions that can modulate hind paw withdrawal responses to noxious heat. To confirm our hind paw withdrawal findings, we conducted experiments using CPP as a measure of antinociception. Reinforcement of behaviors that reduce loss or injury (negative reinforcement) is crucial for survival. Ongoing pain can be "unmasked" in animals using CPP. In the presence of ongoing pain, pairing manipulations that are not rewarding in the absence of pain, such as peripheral nerve block, with a neutral context elicits CPP. Conditioned place preference resulting from pain relief is a measure of negative reinforcement and has previously been shown to be an effective way to concomitantly determine the presence of tonic pain and the effectiveness of agents that relieve it.[21,31]

An important finding from this study was that there is a difference in response to CNO between naive animals and those that had undergone CFA ankle injection. This indicates that RMTg function may change in the context of persistent pain. In the absence of persistent pain, optogenetic inhibition of RMTg GABAergic neurons produced CPP, whereas activation produced conditioned place aversion.[39] In this study, chemogenetic activation of these neurons failed to produce a conditioned place aversion in the context of inflammatory pain. Mechanistically, it is known that VTA and RMTg GABAergic neurons are excited by aversive stimuli, and that activation of these neurons suppresses VTA dopaminergic neuron firing during aversive events.[7] Therefore, in the absence of CFA-induced inflammation, CNO was effective in exciting RMTg GABAergic neurons and produced

increased thermal sensitivity in the Hargreaves test. However, in the context of painful inflammation, aversive stimuli itself trigger RMTg GABAergic neuron excitation through inputs from the lateral habenula,[15] potentially producing a ceiling effect whereby CNO is unable to further excite these neurons, explaining why conditioned place aversion was not seen in the context of persistent pain.

It is possible, and likely, that the antinociceptive effects of RMTg GABAergic neuron inhibition occur through effects on multiple downstream sites, as the RMTg has major projections to the VTA, medial tegmentum, pedunculopontine and laterodorsal tegmental nuclei, dorsal raphe, locus ceruleus, and subceruleus.[16] We elected to study just one of these circuits, that of the RMTg to VTA to NAc. Electrophysiologic recordings obtained from slice preparations showed opioid inhibition of GABA-A IPSCs measured on VTA dopamine neurons was largely due to projections arising from the RMTg.[26] In turn, these VTA neurons modulate dopamine release in the NAc.[14] In this study, we demonstrate the relevance of these in vitro observations for pain-related behaviors. Our FSCV data demonstrate that these neurons modulate dopamine release in the NAc, and the antinociceptive effects of VTA dopamine neuron stimulation are consistent with our hypothesis that RMTg antinociceptive effects are in part mediated through dopaminergic circuits, although we did not confirm that these effects were due to dopamine vs a different transmitter.

Inputs to the NAc arise from the amygdala, thalamus, prefrontal cortex, and anterior cingulate cortex. These inputs are integrated at the level of NAc medium spiny neurons, which in turn project primarily to the ventral pallidum, lateral hypothalamus, and VTA.[43] Many of these input and output regions have been implicated in aversive and/or nociceptive processing.[48] Consequently,

changing the integration of nociceptive or sensory information in the NAc or altering accumbal output to the ventral pallidum/lateral hypothalamus/VTA could all potentially alter pain perception.

Studies investigating the role of DA circuits and pain have largely focused on their contribution to the rewarding effects of opioids.[10,26,44] However, optogenetic activation of VTA dopaminergic neurons also reverses pathological allodynia resulting from nerve injury or bone cancer.[47] In this study, we demonstrate that the hind paw withdrawal response to a noxious heat stimulus in animals with persistent inflammatory pain is also attenuated by selective VTA dopaminergic activation. Preclinical studies in rodents and clinical trials have indicated that dopamine modulators such as D-amphetamine and methylphenidate (MPH) attenuate pain behaviors, are synergistic with opioids, and oppose opioid-induced respiratory depression and sedation.[5,6,11,30] However, the importance of these observations is controversial; although some studies have shown that increasing dopamine activity in humans does not change sensory thresholds,[3] dopamine agonists produce analgesia in Parkinson disease[12,38] and may, therefore, be considered pain modulators. The issue of dopaminergic agonists being analgesic is complex because, aside from sensory processing, the experience of pain also involves complex neural circuits that underlie emotion and motivation.

Changes in the RMTg GABAergic tone produce complex interactions between analgesia, reward, and locomotion in animal models. In contrast to the report of impaired rotarod motor performance associated with KORD-based chemogenetic inhibition of VTA GABAergic interneurons,[1] we observed no effect of chemogenetic inhibition of RMTg GABAergic neurons on rotarod performance. These results highlight that the GABAergic neurons found in the VTA and those that comprise the RMTg are distinct populations with differing functions.[40]

Although this study was the first to chemogenetically manipulate RMTg GABA neurons to assess behavioral pain endpoints, there is extensive literature assessing other behavioral readouts. hM3D and hM4D receptors were expressed in RMTg GABA neurons to investigate locomotion,[46] whereas a novel G_i-coupled, optically sensitive, mu opioid–like receptor expressed in RMTg GABAergic neurons was used to investigate reward.[37] Based on these studies, we predict that our chemogenetic-based results are not specifically related to opioid-mediated inhibition using the KOR-based DREADD and thus could be produced by other techniques including muscimol infusion, hM4d-DREADD, inhibitory opsins, or ablation.

One limitation to this study is the difficulty in definitively identifying RMTg neurons. There are no cytoarchitectural boundaries in Nissl-stained tissue, making its identification heavily reliant on histochemical markers such as the vesicular GABA transporter that was used in the current study. Retrograde labeling from the VTA and psychostimulant-induced c-Fos expression have also been used. However, each of these strategies has limitations. Many neurons immediately adjacent to the RMTg also express GABAergic markers, and retrograde labeling from the VTA does not distinguish the RMTg from adjacent neurons within the VTA itself. Although psychostimulant-induced c-Fos robustly identifies the RMTg in rats, it only labels half of RMTg neurons and is also present in adjacent, non-RMTg cells. A transcription factor, FoxP1, was recently identified as being expressed in GABAergic RMTg neurons.[22] This unique marker was further characterized to show that it is a particularly comprehensive and selective marker of the RMTg.[39] Future studies will be able to make use of these advances.

These results provide compelling behavioral evidence that the RMTg is an important mediator of opioid analgesia, that RMTg GABAergic neurons modulate nociception, and that the mechanism of these RMTg-mediated effects is in part through actions on VTA dopamine neurons. Further studies are needed to better understand the downstream targets of the RMTg and to determine whether the RMTg may be an important site of action for novel, minimally rewarding μ-opioid receptor analgesics.

Conflict of interest statement

The authors have no conflicts of interest to declare.

Appendix A. Supplemental digital content

Supplemental digital content associated with this article can be found online at http://links.lww.com/PAIN/A842.

References

[1] Alexander GM, Rogan SC, Abbas AI, Armbruster BN, Pei Y, Allen JA, Nonneman RJ, Hartmann J, Moy SS, Nicolelis MA, McNamara JO, Roth BL. Remote control of neuronal activity in transgenic mice expressing evolved G protein-coupled receptors. Neuron 2009;63:27–39.

[2] Barrot M, Sesack SR, Georges F, Pistis M, Hong S, Jhou TC. Braking dopamine systems: a new GABA master structure for mesolimbic and nigrostriatal functions. J Neurosci 2012;32:14094–101.

[3] Becker S, Gandhi W, Elfassy NM, Schweinhardt P. The role of dopamine in the perceptual modulation of nociceptive stimuli by monetary wins or losses. Eur J Neurosci 2013;38:3080–8.

[4] Bourdy R, Barrot M. A new control center for dopaminergic systems: pulling the VTA by the tail. Trends Neurosci 2012;35:681–90.

[5] Bruera E, Brenneis C, Paterson AH, MacDonald RN. Use of methylphenidate as an adjuvant to narcotic analgesics in patients with advanced cancer. J Pain Symptom Manage 1989;4:3–6.

[6] Bruera E, Chadwick S, Brenneis C, Hanson J, MacDonald RN. Methylphenidate associated with narcotics for the treatment of cancer pain. Cancer Treat Rep 1987;71:67–70.

[7] Cohen JY, Haesler S, Vong L, Lowell BB, Uchida N. Neuron-type-specific signals for reward and punishment in the ventral tegmental area. Nature 2012;482:85–8.

[8] Dobi A, Margolis EB, Wang HL, Harvey BK, Morales M. Glutamatergic and nonglutamatergic neurons of the ventral tegmental area establish local synaptic contacts with dopaminergic and nondopaminergic neurons. J Neurosci 2010;30:218–29.

[9] Ferreira JG, Del-Fava F, Hasue RH, Shammah-Lagnado SJ. Organization of ventral tegmental area projections to the ventral tegmental area-nigral complex in the rat. Neuroscience 2008;153:196–213.

[10] Fields HL, Margolis EB. Understanding opioid reward. Trends Neurosci 2015;38:217–25.

[11] Forrest WH Jr, Brown BW Jr, Brown CR, Defalque R, Gold M, Gordon HE, James KE, Katz J, Mahler DL, Schroff P, Teutsch G. Dextroamphetamine with morphine for the treatment of postoperative pain. N Engl J Med 1977;296:712–15.

[12] Ha AD, Jankovic J. Pain in Parkinson's disease. Mov Disord 2012;27: 485–91.

[13] Hargreaves K, Dubner R, Brown F, Flores C, Joris J. A new and sensitive method for measuring thermal nociception in cutaneous hyperalgesia. PAIN 1988;32:77–88.

[14] Jalabert M, Bourdy R, Courtin J, Veinante P, Manzoni OJ, Barrot M, Georges F. Neuronal circuits underlying acute morphine action on dopamine neurons. Proc Natl Acad Sci USA 2011;108:16446–50.

[15] Jhou TC, Fields HL, Baxter MG, Saper CB, Holland PC. The rostromedial tegmental nucleus (RMTg), a GABAergic afferent to midbrain dopamine neurons, encodes aversive stimuli and inhibits motor responses. Neuron 2009;61:786–800.

[16] Jhou TC, Geisler S, Marinelli M, Degarmo BA, Zahm DS. The mesopontine rostromedial tegmental nucleus: a structure targeted by the lateral habenula that projects to the ventral tegmental area of Tsai and substantia nigra compacta. J Comp Neurol 2009;513:566–96.

[17] Jhou TC, Xu SP, Lee MR, Gallen CL, Ikemoto S. Mapping of reinforcing and analgesic effects of the mu opioid agonist endomorphin-1 in the ventral midbrain of the rat. Psychopharmacology (Berl) 2012;224: 303–12.

[18] Johnson SW, North RA. Opioids excite dopamine neurons by hyperpolarization of local interneurons. J Neurosci 1992;12:483–8.

[19] Kaufling J, Veinante P, Pawlowski SA, Freund-Mercier MJ, Barrot M. gamma-Aminobutyric acid cells with cocaine-induced DeltaFosB in the ventral tegmental area innervate mesolimbic neurons. Biol Psychiatry 2010;67:88–92.

[20] Keithley RB, Wightman RM. Assessing principal component regression prediction of neurochemicals detected with fast-scan cyclic voltammetry. ACS Chem Neurosci 2011;2:514–25.

[21] King T, Vera-Portocarrero L, Gutierrez T, Vanderah TW, Dussor G, Lai J, Fields HL, Porreca F. Unmasking the tonic-aversive state in neuropathic pain. Nat Neurosci 2009;12:1364–6.

[22] Lahti L, Haugas M, Tikker L, Airavaara M, Voutilainen MH, Anttila J, Kumar S, Inkinen C, Salminen M, Partanen J. Differentiation and molecular heterogeneity of inhibitory and excitatory neurons associated with midbrain dopaminergic nuclei. Development 2016;143:516–29.

[23] Lecca S, Melis M, Luchicchi A, Ennas MG, Castelli MP, Muntoni AL, Pistis M. Effects of drugs of abuse on putative rostromedial tegmental neurons, inhibitory afferents to midbrain dopamine cells. Neuropsychopharmacology 2011;36:589–602.

[24] Lecca S, Melis M, Luchicchi A, Muntoni AL, Pistis M. Inhibitory inputs from rostromedial tegmental neurons regulate spontaneous activity of midbrain dopamine cells and their responses to drugs of abuse. Neuropsychopharmacology 2012;37:1164–76.

[25] Lim G, Kim H, McCabe MF, Chou CW, Wang S, Chen LL, Marota JJ, Blood A, Breiter HC, Mao J. A leptin-mediated central mechanism in analgesia-enhanced opioid reward in rats. J Neurosci 2014;34: 9779–88.

[26] Matsui A, Jarvie BC, Robinson BG, Hentges ST, Williams JT. Separate GABA afferents to dopamine neurons mediate acute action of opioids, development of tolerance, and expression of withdrawal. Neuron 2014; 82:1346–56.

[27] Matsui A, Williams JT. Opioid-sensitive GABA inputs from rostromedial tegmental nucleus synapse onto midbrain dopamine neurons. J Neurosci 2011;31:17729–35.

[28] Milekic MH, Brown SD, Castellini C, Alberini CM. Persistent disruption of an established morphine conditioned place preference. J Neurosci 2006; 26:3010–20.

[29] Mogil JS. Animal models of pain: progress and challenges. Nat Rev Neurosci 2009;10:283–94.

[30] Morgan MJ, Franklin KB. Dopamine receptor subtypes and formalin test analgesia. Pharmacol Biochem Behav 1991;40:317–22.

[31] Navratilova E, Xie JY, Okun A, Qu C, Eyde N, Ci S, Ossipov MH, King T, Fields HL, Porreca F. Pain relief produces negative reinforcement through activation of mesolimbic reward-valuation circuitry. Proc Natl Acad Sci USA 2012;109:20709–13.

[32] Paxinos G, Franklin KBJ, Franklin KBJ. The mouse brain in stereotaxic coordinates. San Diego: Academic Press, 2001.

[33] Perrotti LI, Bolanos CA, Choi KH, Russo SJ, Edwards S, Ulery PG, Wallace DL, Self DW, Nestler EJ, Barrot M. DeltaFosB accumulates in a GABAergic cell population in the posterior tail of the ventral tegmental area after psychostimulant treatment. Eur J Neurosci 2005;21:2817–24.

[34] Phillips PE, Robinson DL, Stuber GD, Carelli RM, Wightman RM. Real-time measurements of phasic changes in extracellular dopamine concentration in freely moving rats by fast-scan cyclic voltammetry. Methods Mol Med 2003;79:443–64.

[35] Prabhakar S, Taherian M, Gianni D, Conlon TJ, Fulci G, Brockmann J, Stemmer-Rachamimov A, Sena-Esteves M, Breakefield XO, Brenner GJ. Regression of schwannomas induced by adeno-associated virus-mediated delivery of caspase-1. Hum Gene Ther 2013;24:152–62.

[36] Samineni VK, Grajales-Reyes JG, Copits BA, O'Brien DE, Trigg SL, Gomez AM, Bruchas MR, Gereau RW. Divergent modulation of nociception by glutamatergic and GABAergic neuronal subpopulations in the periaqueductal gray. eNeuro 2017;4: ENEURO.0129-16.2017.

[37] Siuda ER, Copits BA, Schmidt MJ, Baird MA, Al-Hasani R, Planer WJ, Funderburk SC, McCall JG, Gereau RW, Bruchas MR. Spatiotemporal control of opioid signaling and behavior. Neuron 2015;86:923–35.

[38] Skogar O, Lokk J. Pain management in patients with Parkinson's disease: challenges and solutions. J Multidiscip Healthc 2016;9:469–79.

[39] Smith RJ, Vento PJ, Chao YS, Good CH, Jhou TC. Gene expression and neurochemical characterization of the rostromedial tegmental nucleus (RMTg) in rats and mice. Brain Struct Funct 2019;224:219–38.

[40] Steidl S, Wasserman DI, Blaha CD, Yeomans JS. Opioid-induced rewards, locomotion, and dopamine activation: a proposed model for control by mesopontine and rostromedial tegmental neurons. Neurosci Biobehav Rev 2017;83:72–82.

[41] Stein C, Clark JD, Oh U, Vasko MR, Wilcox GL, Overland AC, Vanderah TW, Spencer RH. Peripheral mechanisms of pain and analgesia. Brain Res Rev 2009;60:90–113.

[42] Stuber GD, Roitman MF, Phillips PE, Carelli RM, Wightman RM. Rapid dopamine signaling in the nucleus accumbens during contingent and noncontingent cocaine administration. Neuropsychopharmacology 2005;30: 853–63.

[43] Thompson JM, Neugebauer V. Cortico-limbic pain mechanisms. Neurosci Lett 2019;702:15–23.

[44] Trang T, Al-Hasani R, Salvemini D, Salter MW, Gutstein H, Cahill CM. Pain and poppies: the good, the bad, and the ugly of opioid analgesics. J Neurosci 2015;35:13879–88.

[45] Wang D, Tawfik VL, Corder G, Low SA, Francois A, Basbaum AI, Scherrer G. Functional divergence of delta and mu opioid receptor organization in CNS pain circuits. Neuron 2018;98:90–108 e105.

[46] Wasserman DI, Tan JM, Kim JC, Yeomans JS. Muscarinic control of rostromedial tegmental nucleus GABA neurons and morphine-induced locomotion. Eur J Neurosci 2016;44:1761–70.

[47] Watanabe M, Narita M, Hamada Y, Yamashita A, Tamura H, Ikegami D, Kondo T, Shinzato T, Shimizu T, Fukuchi Y, Muto A, Okano H, Yamanaka A, Tawfik VL, Kuzumaki N, Navratilova E, Porreca F, Narita M. Activation of ventral tegmental area dopaminergic neurons reverses pathological allodynia resulting from nerve injury or bone cancer. Mol Pain 2018;14: 1744806918756406.

[48] Wulff AB, Tooley J, Marconi LJ, Creed MC. Ventral pallidal modulation of aversion processing. Brain Res 2019;1713:62–9.